Disproportionation of thermoelectric bismuth telluride nanowires as a result of the annealing process†‡

Jongmin Lee,[abc] Andreas Berger,[c] Laurent Cagnon,[d] Ulrich Gösele,[c] Kornelius Nielsch*[e] and Jaeyoung Lee*[ab]

Received 31st May 2010, Accepted 28th October 2010
DOI: 10.1039/c0cp00749h

P-type thermoelectric bismuth telluride nanowires were fabricated by pulsed electrodeposition in anodic aluminium oxide (AAO) membranes. Subsequently, the nanowires were annealed at 423, 523 and 673 K in an inert atmosphere for 4 h. With increasing temperature, it was observed that the Te compound incongruently sublimates due to its high vapor pressure, leading to disproportionation (from Bi_2Te_3 to Bi_4Te_3 *via* Bi_4Te_5). The crystalline structure of the nanowires was then investigated using XRD and SAED, with nanowire compositions investigated using an EDX attached to a TEM. The crystallinity of the nanowires was found to be enhanced with increased annealing temperature, and nanowires annealed at 673 K were stably maintained in the Bi_4Te_3 phase. Additionally, the Seebeck coefficient was determined and the thermopower of nanowires annealed at a temperature of 423 K was shown to be slightly enhanced. Significantly suppressed Seebeck values for annealing temperatures of 523 K and 673 K were also observed.

Introduction

In the future, thermoelectric materials are positioned to play an increasing role in the efficient use of energy. Thermoelectric materials can be utilized as electric generators or coolers for several purposes, such as power generation in automotive applications and microcoolers,[1] and also for infrared detectors.[2] The thermoelectric efficiency of a material is characterized by a dimensionless figure of merit $ZT = \frac{S^2\sigma T}{\kappa}$, where S is the Seebeck coefficient, σ is the electrical conductivity, κ is the thermal conductivity, and T is the absolute temperature.[3] To date, a number of approaches have attempted to enhance the thermoelectric efficiency; many recent advances in increasing the figure of merit are linked to nanoscale phenomena found both in bulk samples containing nanoscale constituents as well as in the nanoscale samples themselves.[4] For example, $AgPb_mSbTe_{2+m}$ showed an impressively high ZT of $\sim$2.2 at 800 K owing to embedded nanostructured precipitates.[5] The highest ZT reported to date ($\sim$2.4) was measured in Bi_2Te_3/Sb_2Te_3 superlattice films.[6] Regarding a low-dimensional system approach, however, the internal interfaces found in nanostructures need to be designed in such a way that the thermal conductivity is reduced. This approach originates *via* the strong suppression of phonon-based contributions of the thermal conductivity, whereas the electrical conductivity is ideally kept unaffected.[7] Furthermore, it has also been reported that annealing processes can be successfully applied to optimize the thermoelectric performance.[8–10] As such, annealing can be used to alter the defect concentration of materials, leading to a modification of the carrier concentration.

In this article, we investigate the disproportionation in Bi_2Te_3 nanowires during the annealing process in an Ar atmosphere, and thereby increase our understanding of the effect of annealing on the thermoelectric performance. Previously, Wang *et al.*[11] reported that the spontaneous formation of Bi_2Te_3/Te heterostructured nanowires occurred during the annealing of a supersaturated $Bi_{0.26}Te_{0.74}$ alloy. In contrast, we demonstrate here the incongruent sublimation of the Te compound during the annealing process, leading to extremely Bi-rich Bi–Te nanowires, in addition to a significant reduction of the Seebeck coefficient due to the development of a strongly metallic Bi–Te compositional alloy.

Experimental section

Anodic aluminium oxide (AAO) membranes were prepared using a two-step anodization process in 0.3 M oxalic acid at an applied voltage of 40 V; a more detailed description of the fabrication procedure can be found in ref. 12. Bismuth telluride nanowires were fabricated by pulsed potential electrodeposition with a 50 ms off time (5 ms on time) until an overgrown film covered the top surface of the AAO, as reported in our previous paper.[13] The diameter of the nanowires was the same as for AAO (50 nm) and the nanowires reached a length of 25 μm. After nanowire growth in the nanochannel structure of

[a] *Ertl Center for Electrochemistry and Catalysis, Gwangju Institute of Science and Technology, Gwangju 500-712, South Korea. E-mail: jaeyoung@gist.ac.kr; Fax: +82-62-970-2434; Tel: +82-62-970-2571*
[b] *School of Environmental Science and Engineering, Gwangju Institute of Science and Technology, Gwangju 500-712, South Korea*
[c] *Max Planck Institute of Microstructure Physics, D-06120 Halle, Germany*
[d] *Institut Néel, CNRS et Université Joseph Fourier, F-38042 Grenoble Cedex 9, France*
[e] *Institute of Applied Physics, University of Hamburg, D-20355 Hamburg, Germany. E-mail: knielsch@phsik.uni-hamburg.de*

† Contributed to the PCCP collection on Electrified Surface Chemistry, following the 1st Ertl Symposium on Electrochemistry and Catalysis, 11–14 April, 2010, Gwangju, South Korea.

‡ Electronic supplementary information (ESI) available: Morphology and compositional variations of the overgrown Bi–Te film and XRD patterns of annealed Bi–Te nanowires. See DOI: 10.1039/c0cp00749h

AAO, nanowires within the alumina matrix were annealed at different temperatures (423 K, 523 K, and 673 K). The annealing process was performed under a controlled Ar atmosphere at 2 mbar pressure for 4 h. Prior to the annealing process, a pre-flow was sustained for 30 min in order to eliminate possible contamination on the tubular chamber walls. The morphologies of the nanowires and the overgrown film were then investigated *via* scanning electron microscopy (SEM), and the crystalline structure of the nanowires was investigated by X-ray diffraction (XRD), high-resolution transmission electron microscopy (HRTEM), and selected area electron diffraction (SAED) patterns. In addition, the composition of the nanowires was investigated using an energy dispersive X-ray spectroscope (EDX) attached to the TEM system. For this analysis step, the fabricated nanowires were dispersed on TEM grids after selective dissolution of the alumina matrix in 2 M NaOH.

To measure the Seebeck coefficient, an Au layer was sputtered onto the front side of the membrane through a circular mask (1 mm diameter) after mechanical removal of the overgrown bismuth telluride (Bi–Te) film by ion-milling. This step ensured an enhanced electrical and thermal contact between the nanowire array and the copper blocks of the measurement setup. The Au layer had to be deposited carefully in order to prevent an Au coating from accumulating on the sample edges, which could cause short circuits. For the thermopower measurements, the samples were placed between two copper blocks and a constant temperature gradient of 15 K was applied.

Results and discussion

In these experiments, mixed bismuth and tellurium oxide (Bi_2O_3 and TeO_2) layers were observed to form a shell structure, as shown in Fig. 1(a). Note that the oxygen intensity fluctuates at positions 4 and 24 on the *x*-axis (the interfaces at both sides of the nanowires). This fluctuation indicates Bi_2O_3 and TeO_2 layers formed on the outer surface of the nanowires as a shell structure during the annealing process.

In a previous report by Menke *et al.*,[14] X-ray photoelectron spectroscopy (XPS) data for freshly prepared nanowires found that they were quickly covered by mixed bismuth and tellurium oxides, resulting from air oxidation at the surface of the Bi_2Te_3 nanowires. Then, based on the layered oxide structure model suggested by Bando *et al.*,[15] it is estimated that within 1 h of air exposure the oxide structure consists of layers of Bi_2O_3 and TeO_2 that are 2.2 and 1.1 nm thick, respectively. As shown in Fig. 1(b), as the annealing temperature increases, the atomic ratio (Te/Bi) tends to decrease due to the reduction of the Te compound, similar to the previous EDX data for overgrown film, (see Supporting Information‡) leading to a Bi-rich Bi–Te nanowire structure. The composition of the as-prepared nanowires and the nanowires annealed at 423 K is close to Bi_2Te_3; however, a transformation from Bi_2Te_3 into Bi_4Te_5 (523 K) and Bi_4Te_3 (673 K) was observed with an increasing annealing temperature. This transformation is caused by the higher vapor pressure of Te compared to Bi, leading to a higher evaporation rate of the Te compound, as presented in the vapor pressure graph and Bi–Te alloy phase diagram.[16,17]

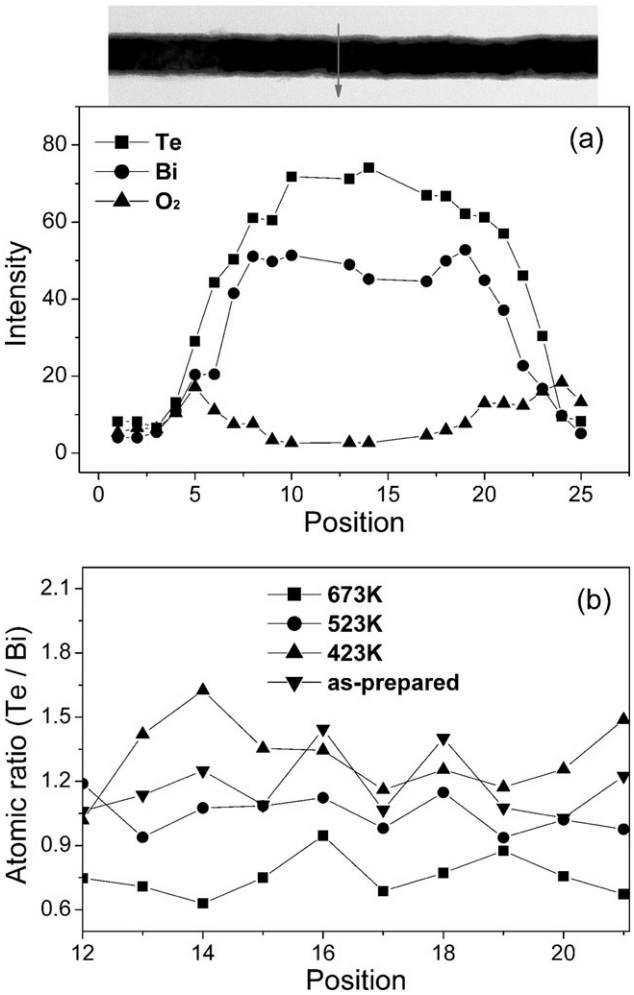

Fig. 1 (a) Representative intensity profiles of elements for individual nanowires annealed at 423 K and (b) atomic ratio (Te/Bi) variations of individual nanowires annealed at different temperatures. Note that the data was confirmed by EDX coupled with a TEM system performing a line scan across the nanowire.

In addition, the high surface area would also affect the evaporation rate in the nanowire system.

Most notably, several black spots (crystallites) were observed in the bismuth telluride nanowires annealed at 523 K. Therefore, line scans were performed with a particular focus on this area, as shown in Fig. 2; in Fig. 2(a), the intensity of the bismuth decreased significantly at a certain point, whereas the intensity of Te increased. This result is decisive evidence that the crystallite composition was relatively pure Te. In addition, the much higher atomic ratio ($\sim$6) supports the hypothesis that the black spots consisted of pure Te. However, with a further increase of the annealing temperature to 673 K, the black spots were no longer observed, indicating that the Te crystallites had decomposed during the annealing process due to the high vapor pressure of Te.[16]

Moreover, the atomic ratio of the annealed nanowires also decreased (Fig. 1(b)). Unlike the complete separation of the Bi_2Te_3/Te multi-structure reported by Wang *et al.*[11] however, the Te crystallites formed irregularly along the annealed nanowire axis, which showed a stronger rate of evaporation

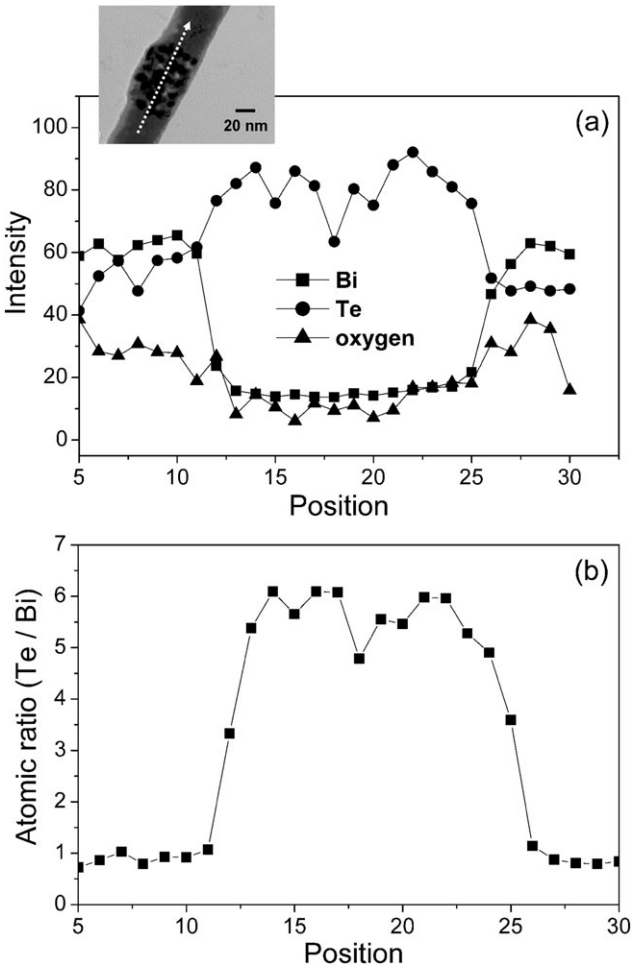

Fig. 2 EDX of a nanowire annealed at 523 K: (a) intensity of each element, and (b) atomic ratio (Te/Bi) of the nanowire. Note that the line scan was performed inside the nanowire.

of the Te element at increasing annealing temperature. The crystalline structure and the transformation of the annealed nanowires were then revealed by XRD (see Supporting Information‡) and SAED patterns.

Fig. 3 shows the SAED patterns of nanowires annealed at different temperatures. For the nanowires annealed at 423 K, the SAED pattern consisting of bright spots indicates the single crystalline structure of the nanowire, which can be indexed at (205), (110), and (0015) in hexagonal Bi_2Te_3 phase (rhombohedral ($R\bar{3}m$) space group). Additionally, the growth direction of this nanowire is along the *c*-axis [0 0 *l*] perpendicular to the nanowire. With an increase in the annealing temperature to 523 K, the SAED shows a ring pattern, indicating the polycrystalline nature of the nanowires. The main reason for this change is structure might be the mixture of a Bi_4Te_5 phase (rhombohedral ($R\bar{3}m$) space group) and Te phase crystallites, consistent with the previous results (EDX and XRD). In addition, the indexes (0011) and (0027) were observed in the corresponding SAED pattern, with *c*-axis growth similar to the bismuth telluride nanowires annealed at 423 K. At the final stage of the annealing process, the SAED patterns of nanowires annealed at 623 K again display a single crystalline structure. This enhancement of the nanowire crystal quality can be explained by the recrystallization of Te crystallites and subsequent transformation to a more stable Bi–Te phase (Bi_4Te_3), according to the binary alloy Bi–Te phase diagram.[17] In a previous report,[18] Bi_4Te_3 nanowires grown by molecular beam epitaxy (MBE) at 600 K were achieved as a stable state. Also, the viewing zone axes for the Bi_4Te_3 nanowires were determined to be [110] and [1121], with *c*-axis growth with the rhombohedral ($R\bar{3}m$) space group.

Fig. 4 shows the Seebeck coefficient of the Bi–Te nanowires as a function of the annealing temperatures. The measured Seebeck coefficients were positive, indicating a *p*-type characteristic, which are likely due to an excess of Bi component. As the annealing temperature was increased to 423 K, the Seebeck coefficient rose slightly from 53 $\mu V\ K^{-1}$ (as-prepared) to 57 $\mu V\ K^{-1}$. This slight enhancement of Seebeck coefficient could be attributed to the improved crystal quality due to annealing effects, rather than the carrier concentration of the nanowire. However, it significantly decreased to 19 $\mu V\ K^{-1}$ (64% reduction) and then recovered to 29 $\mu V\ K^{-1}$ with a further increase in temperature. Similar results have been previously reported. Bailini *et al.*[19] presented Seebeck coefficient variations of Bi_2Te_3, BiTe, and Bi_4Te_3 films; in their results, the coefficients significantly decreased from $-175\ \mu V\ K^{-1}$ (Bi_2Te_3) to $-75\ \mu V\ K^{-1}$ (Bi_4Te_3). Though the reduction of the Seebeck coefficient with increasing annealing temperature is presently not well understood, a hypothesis can be suggested. The unbalanced composition of nanowires would reduce the Seebeck coefficient due to the loss of the Te element, as the surface-to-volume ratio is quite high in 1D nanostructures. Therefore, the composition of nanowires can be easily modified during the annealing process at certain temperatures. Consequently, it is well known that the Seebeck coefficient is inversely proportional to the carrier

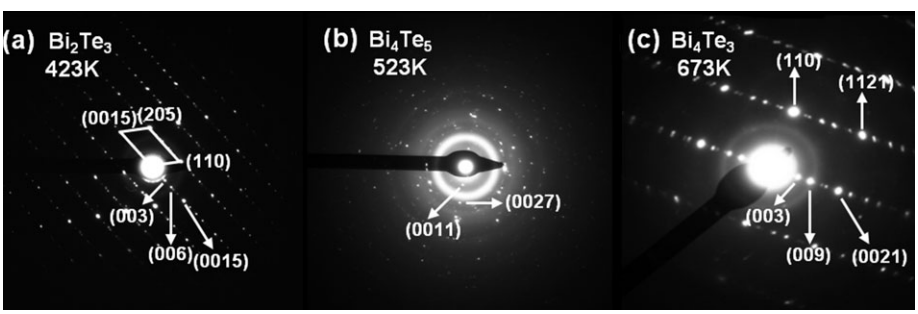

Fig. 3 Selected area electron diffraction (SAED) patterns of annealed nanowires at different temperatures: (a) 423 K, (b) 523 K, and (c) 673 K.

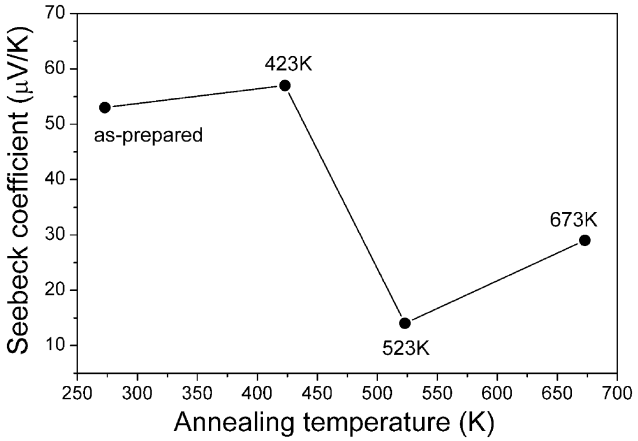

Fig. 4 Seebeck coefficient variations of Bi_2Te_3 nanowires as a function of the annealing temperature.

concentration,[20] *i.e.*, the carrier concentration would grow with rising annealing temperature because of increasing Te deficiency. In addition, the slight enhancement of the Seebeck coefficient at a 673 K annealing temperature can also be attributed to the improved crystal quality of the nanowires.

Conclusions

Thermoelectric Bi–Te nanowires fabricated by pulsed electrodeposition were annealed for 4 h in an Ar atmosphere at set temperatures of 423 K, 523 K, and 673 K. The annealed nanowires showed a good single-crystalline structure, except for the specimen annealed at 523 K. The as-prepared nanowires consisted of a Bi_2Te_3 phase, which transformed into Bi_4Te_5 and Bi_4Te_3 with increasing annealing temperatures. Due to the much higher vapor pressure of Te at a given temperature, loss of the Te element occurred. In particular, irregular Te crystallites were observed in nanowires annealed at 523 K, leading to a polycrystalline structure of the nanowires with Bi_4Te_5. These nanowires were then recrystallized and continuously vaporized at a further increased annealing temperature (673 K). Accordingly, the Seebeck coefficients slightly increased at an annealing temperature of 423 K and significantly decreased at 523 K, though slightly recovered at 673 K. The slight enhancement of the Seebeck coefficient could be attributed to the improved crystal quality of the nanowires, and the reduction is mainly due to the unbalanced composition of the nanowires from loss of the Te element. Based on the Seebeck coefficient results, it is expected that Bi–Te based thermoelectric devices will be less efficient in temperatures below 500 K.

Acknowledgements

We gratefully acknowledge Mr. William Töllner (University of Hamburg) for assistance in English writing, and financial support from the German Ministry for Education and Research (BMBF) through the projects 03N8701 and 03X5519, and the German Priority program SPP 1386 on Nanostructured Thermoelectrics funded by the German Science Foundation and the International Max Planck Research School (IMPRS).

References

1 D. M. Rowe and C. M. Bhandari, *Modern Thermoelectrics*, Reston, VA, 1983.
2 G. Min and D. M. Rowe, *Solid-State Electron.*, 1999, **43**, 923.
3 G. S. Nolas, J. Sharp and H. J. Goldsmid, *Thermoelectrics: Basic Principles and New Materials Developments*, Springer, New York, 2001.
4 M. S. Dresselhaus, G. Chen, M. Y. Tang, R. Yang, H. Lee, D. Wang, Z. Ren, J. P. Fleurial and P. Gogna, *Adv. Mater.*, 2007, **19**, 1043.
5 E. Quarez, K. F. Hsu, R. Pcionek, N. Frangis, E. K. Polychroniadis and M. G. Kanatzidis, *J. Am. Chem. Soc.*, 2005, **127**, 9177.
6 R. Venkatasubramanian, E. Siivola, T. Colpitts and B. O'Quinn, *Nature*, 2001, **413**, 597.
7 G. Chen, *Phys. Rev. B: Condens. Matter Mater. Phys.*, 1998, **57**, 14958.
8 O. Yamashita and S. Sugihara, *J. Mater. Sci.*, 2005, **40**, 6439.
9 D. M. Lee, C. H. Lim, D. C. Cho, Y. S. Lee and C. H. Lee, *J. Electron. Mater.*, 2006, **35**, 360.
10 S. Li, H. M. A. Soliman, J. Zhou, M. S. Toprak, M. Muhammed, D. Platzek, P. Ziolkowski and E. Mueller, *Chem. Mater.*, 2008, **20**, 4403.
11 W. Wang, X. Lu, T. Zhang, G. Zhang, W. Jiang and X. Li, *J. Am. Chem. Soc.*, 2007, **129**, 6702.
12 H. Masuda and K. Fukuda, *Science*, 1995, **268**, 1466.
13 J. Lee, S. Fahrangfar, J. Lee, L. Cagnon, R. Scholz, U. Goesele and K. Nielsch, *Nanotechnology*, 2008, **19**(36), 365701.
14 E. J. Menke, M. A. Brown, Q. Li, J. C. Hemminger and R. M. Penner, *Langmuir*, 2006, **22**, 10564.
15 H. Bando, K. Koizumi, Y. Oikawa, D. Daikohara, V. A. Kulbachinskii and H. J. Ozaki, *J. Phys.: Condens. Matter*, 2000, **12**, 5607.
16 http://www.veeco.com/promos/vapor-pressure-curves-of-the-elements.aspx.
17 B. Massalski Tadeusz and H. Okamoto, *Binary alloy phase diagrams*, American Society for Metals (ASM) International, Materials Park, Ohio, 1990.
18 G. Wang, S. K. Lok, G. K. L. Wong and I. K. Sou, *Appl. Phys. Lett.*, 2009, **95**, 263102.
19 A. Bailini, F. Donati, M. Zamboni, V. Russo, M. Passoni, C. S. Casari, A. Li Bassi and C. E. Bottani, *The Proceedings of the 5th European Conference on Thermoelectrics*, ICT 2007, No. 12.
20 *Thermoelectric Handbook (Macro to Nano)*, ed. D. M. Rowe, CRC/Taylor & Francis, New York, 2006.

